G12V Kras mutations in cervical cancer under virtual microscope of molecular dynamics simulations

X.P. Chen[1], W.H. Xu[1], D.F. Xu[2], S.M. Fu[1], Z.C. Ma[1]

[1] *Central Laboratory, The People's Hospital of Hainan Province, Haikou*
[2] *Department of Hepatobilia, The People's Hospital of Hainan Province, Haikou (China)*

Summary

Kras mutations and cancers are common and their role in the progression of cancer is well known and elucidated. The present work is searching for the most deleterious mutation of the four found at codon 12 and 13 of Kras in cervical cancers using prediction servers; different servers were used to look into different factors that govern the protein function. The in silico results predicted G12V to be the most devastating; this particular mutation was then subjected to molecular dynamics simulation (MDS) for further analysis. The authors' approach of MDSs helped them to place the native and mutant structure under virtual microscope and observe their dynamics over time. The results generated are enlightening the effect of G12V variation on the dynamics of Kras. The structural variation between the native and mutant Kras over 50 nanoseconds (ns) run varied at every parameter checked and the results are in excellent agreement with the available experimental data.

Key words: Cervical cancer; Kras; Mutation; Molecular dynamics simulations.

Introduction

With 580,000 cases and 266,000 deaths in 2012, cervical cancer is the second deadliest cancer in women. The disease is more prevalent in less developed regions of the world, estimating around 84% of the total cases and 88% of the total deaths [1]. The incidences of cervical cancer are on alarming rise from 5% to 24% globally [2]. In China the occurrence of cervical cancer is still high in comparison to rest of the world [3], particularly in young women [4]. Ninety-percent of the cervical cancer cases are associated with human papillomavirus (HPV) infection [5].

The mutations in Kras and cancers are common and cervical cancer is not devoid of this phenomenon [6-13]. Studies have investigated the coexistence of HPV and Kras mutations [14], the mutations of Kras are associated with progression of cervical cancer [15]. Kras, a 21 kDa oncoprotein is located at chromosome 12 and exhibits GTPase activity which is needed for cell cycle regulation [16]. Codon 12 and 13 have been reported extensively to be mutated in cervical cancer [17-21].

The present authors' aim in this study was to find the most destructive mutation in Kras at codon 12 and 13, and to use molecular dynamics simulation simulations (MDS) tool to study the dynamics of the shortlisted mutation. To achieve this they used various polymorphism effect prediction servers available online: SIFT [22], Polyphen-2 [23], PhD-SNP [24], and MutPred [25]. The most deleterious mutation was subjected to MDS, a tool that has become a backbone of understanding the effect of mutation.

Materials and Methods

Datasets

The crystal structures of wildtype Kras having PDB ID: 4LUC [26] from Protein Data Bank were used for this investigation. Four mutations G12A, G12D, G12V, and G13D, known to be present in cervical cancers, were selected for polymorphism damage prediction.

Polymorphism damage prediction

Four in silico tools were selected meticulously in order to assess each factor and double-checked other tools which use different algorithms. The details of the servers that were used in the present study are described in Table 1, where the algorithm, basis, and criteria for selection are given.

MDS

The top deleterious mutation was subjected to MDS. The MDS studies were performed by Gromacs 4.5.3 package [27]. For wt Kras, the modeled structure was used as a starting structure for MDS and the Accelrys Discovery Studio [28] was used to make single point mutation on the wild type structure. Both the structures were applied with GROMOS96 43a1 force field and then placed in a model of a pre-equilibrated water bath as shown in Figure 1, and counter-ions were added to achieve a neutral box using the "genion" tool that accompanies with gromacs package. The solvent molecules were restrained to the original position with a force constrain of 100 Kcal/mol for 5,000 steps before being subjected to energy minimization for 5,000 iteration. For regulating the temperature inside the box, Berendsen temperature coupling method [29] was used. Electrostatic interactions were computed using the Particle Mesh Ewald method [30]. The ionizing state of the residues, the pressure, and other parameters were set in the standard range. The non-bonded pair list was updated every ten steps and conformations were stored every two pico sec-

Table 1. — *Different online servers and their related general information.*

Method	Algorithm	Based on	Criteria	Website
SIFT	Alignment scores	Sequence alignment	0 - 0.05 (intolerant)	http://sift.jcvi.org/www/SIFT_enst_submit.html
Phd-SNP	Support vector machine	Sequence and profile information	Disease probability (if $p > 0.5$ mutation is predicted disease)	http://snps.path.uab.edu/phd-snp/phd-snp.html
MutPred	Random forest	SIFT and gain/loss of functions	Scores with $g > 0.5$ and $p < 0.05$ are referred to as actionable hypotheses	http://mutpred.mutdb.org/
Polyphen-2	Bayesian classification	Physical and comparative considerations	Score ≥ 0.5	http://genetics.bwh.harvard.edu/pph2/

Table 2. — *Results generated by the servers.*

Method	G12A	G12D	G12V	G13D
SIFT	DAMAGING (0.4)	DAMAGING (0.12)	DAMAGING (0.01)	DAMAGING (0.2)
Phd-SNP	DISEASE (6)	DISEASE (9)	DISEASE (9)	DISEASE(8)
MutPred	Loss of ubiquitination at K16 ($p = 0.1191$) Loss of methylation at K16 ($p = 0.136$) Loss of stability ($p = 0.2599$) Loss of sheet ($p = 0.302$) Loss of disorder ($p = 0.3361$)	Loss of catalytic residue at G10 ($p = 0.0752$) Gain of ubiquitination at K16 ($p = 0.1181$) Loss of methylation at K16 ($p = 0.1388$) Loss of sheet ($p = 0.302$) Gain of solvent accessibility ($p = 0.4067$)	Loss of catalytic residue at V14 ($p = 0.1046$) Loss of ubiquitination at K16 ($p = 0.1037$) Loss of methylation at K16 ($p = 0.1785$) Loss of disorder ($p = 0.1841$) Loss of sheet ($p = 0.302$) Loss of relative solvent accessibility ($p = 0.3919$)	Loss of ubiquitination at K16 ($p = 0.1191$) Loss of methylation at K16 ($p = 0.1236$) Gain of solvent accessibility ($p = 0.154$) Loss of loop ($p = 0.2237$)
Polyphen-2	POSSIBLY DAMAGING (0.956)	POSSIBLY DAMAGING (0.961)	POSSIBLY DAMAGING (0.999)	POSSIBLY DAMAGING (0.803)

onds (ps). Position restraint simulation for 500 ps was implemented to allow solvent molecules to enter the cavity region of structure. Finally, system was subjected to MDS for 50 nanoseconds (ns). Root mean square deviation (RMSD), root mean square fluctuation (RMSF), radius of gyration (Rg), and principal component analysis (PCA) were carried out by using inbuilt gromacs tools. g-hbond was used to calculate number of distinct hydrogen bonds formed by specific residues to other amino acids within the protein during the simulation (NH bond). g_sham was used extensively used to obtain free energy landscape. The graphs were plotted using Grace GUI toolkit 5.1.22 version. The free energy landscapes were plotted using gnuplot 4.6.0 version. All the visualizations were carried out using Pymol, Ligplus, VMD [31] and graphs were plotted using Grace Program [32] and gnuplot. The trajectories were analyzed using the inbuilt tool in the GROMACS distribution.

Results and Discussion

As we are aware, predicting the possibility of polymorphism to be disease-associated is difficult, because of the fact that an amino acid substitution can affect the gene product i.e. protein in a number of ways. The variation can be in structure, stability of protein, disruption in catalytic site, and various other such factors. Thus the present authors' aim to use different tools for damage prediction was to look into different factors that govern the protein func-
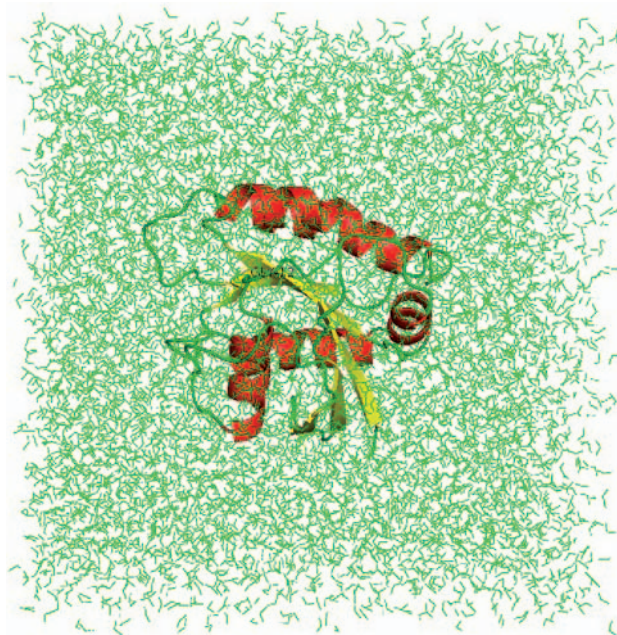

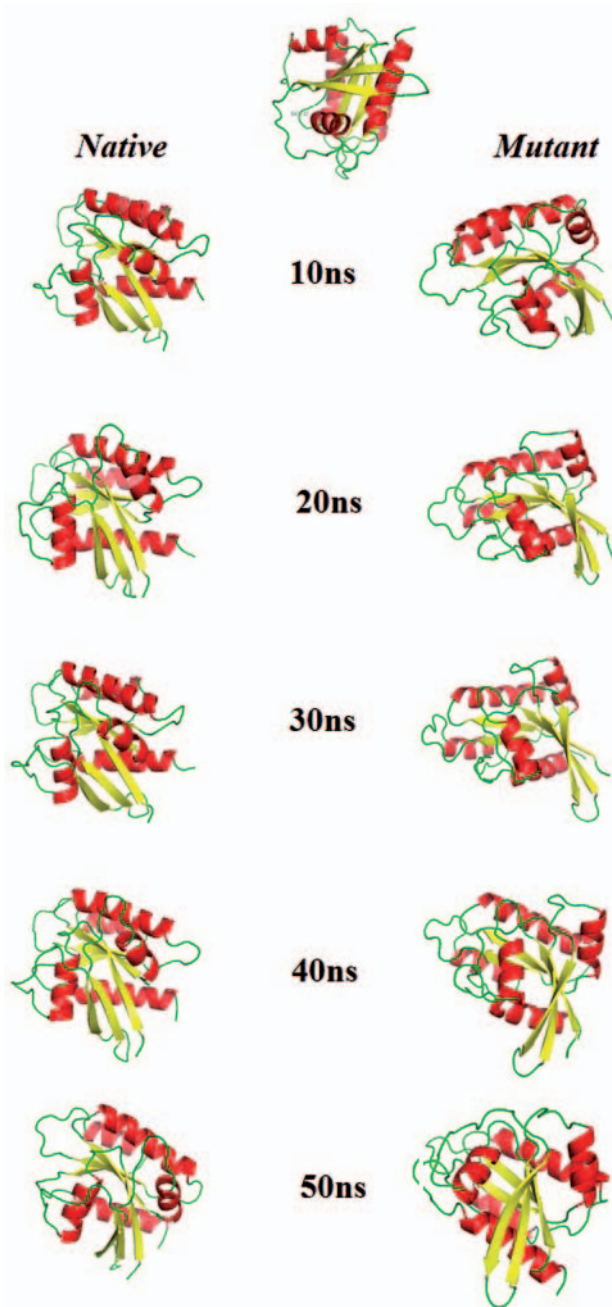Figure 1. — Kras protein in pre-equilibrated water bath and ions.

Figure 2. — Snapshots of native and mutant Kras at different intervals of time.
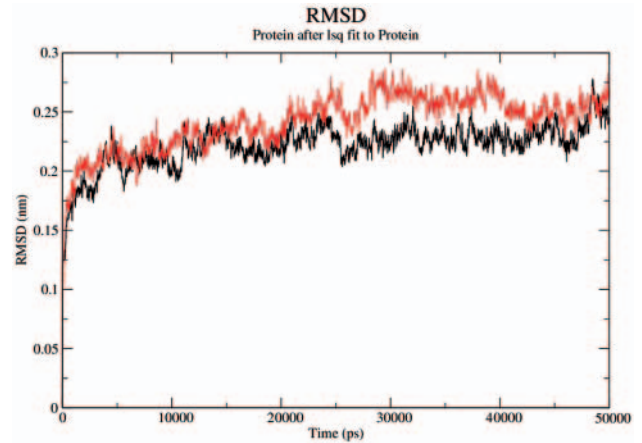

Figure 3. — RMSD changes in native and mutant structures throughout simulations (native is shown in black and mutant in red).

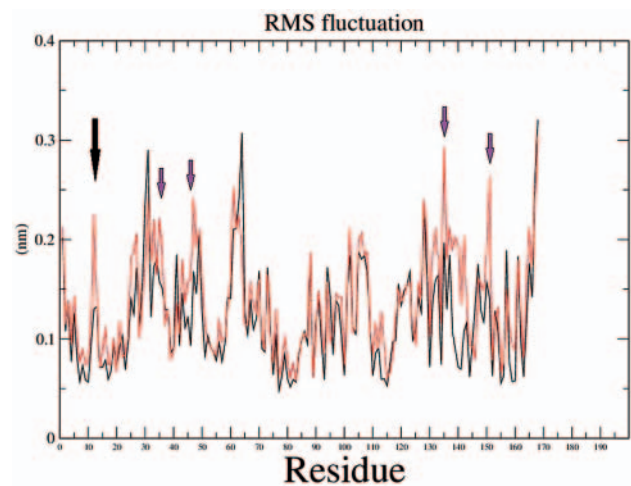Figure 4. — RMSF of all the residues of native and mutant Kras protein at 300 K (native is shown in black and mutant in red).

tion. The tools used were pivotal in limiting this study to mere one most significant deleterious polymorphism. The servers used combinedly reported polymorphism to be disease-associated. The missense mutation of G12V was found to be extremely deleterious (Table 2) in comparison to other three on all the utilized servers.

The MDS approach to study the effect of the G12V deleterious mutation on Kras was successful in elucidating the effects at microscopic level. Figure 2 shows the difference between the two structures at different intervals of time during the simulations, demarking the effect of mutations in general. To investigate the happenings, further Gromacs inbuilt tools g_rms, g_rmsf, g_ gyrate, g-covar and g_anaeig were used. g_rmsf gave the RMSD (root mean square deviation) value curves of Kras in the mutant and native systems during the simulations, Figure3 represents RMSD fluctuations of both native and mutant structures over 50,000 ps, i.e. 50 ns. The analysis is indicating that mutation at codon 12 from G to V is effecting the conformation of the Kras, with mutant structure showing more deviation pattern than native in general.

g_rmsf was used to calculate the atomic standard deviation. Observing RMSF values from Figure 4, it is evident that mutation at codon 12 is making the structure more fluc-

(a)

Radius Of Gyration

(a)

Intra-Protein

(b)

Radii Of Gyration

(b)

Protein-water

(c)

Radii Of Gyration

Figure 6. — (a) Average number of intermolecular hydrogen bonds in native and mutant Kras protein versus time at 300 K. (b) Average number of protein –solvent hydrogen bonds in native and mutant Kras protein versus time at 300 K (native is shown in black and mutant in red).
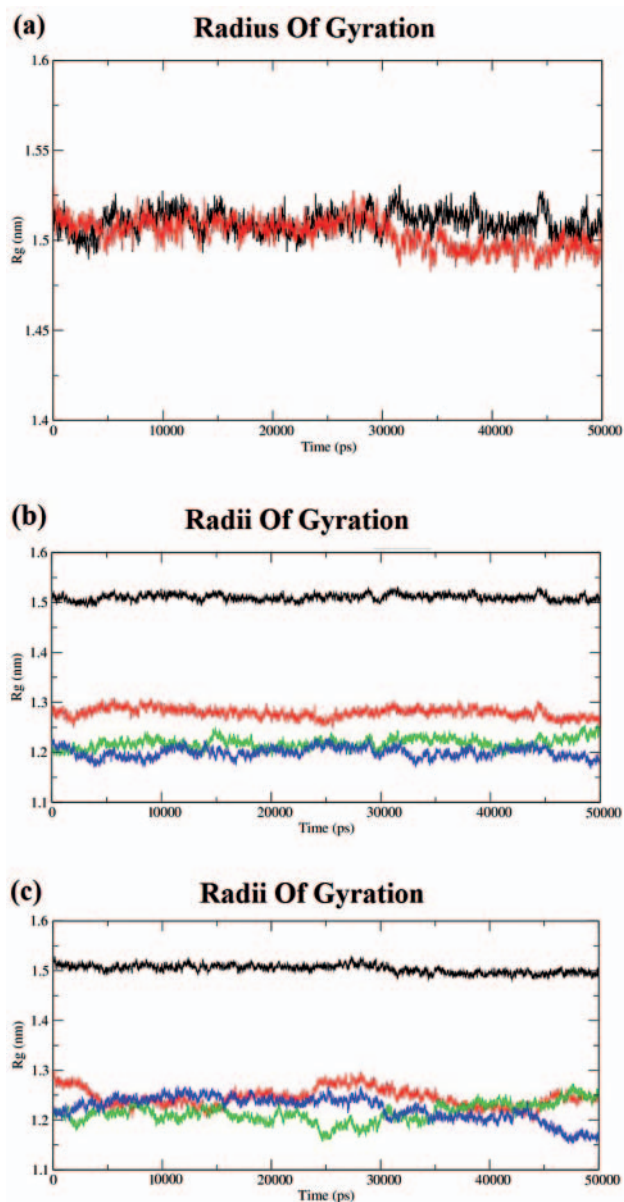
Figure 5. — (a) Radius of gyration of native and mutant Kras protein versus time at 300 K. (b) Radii of gyration of native Kras structure (c) Radii of gyration of mutant Kras structure.
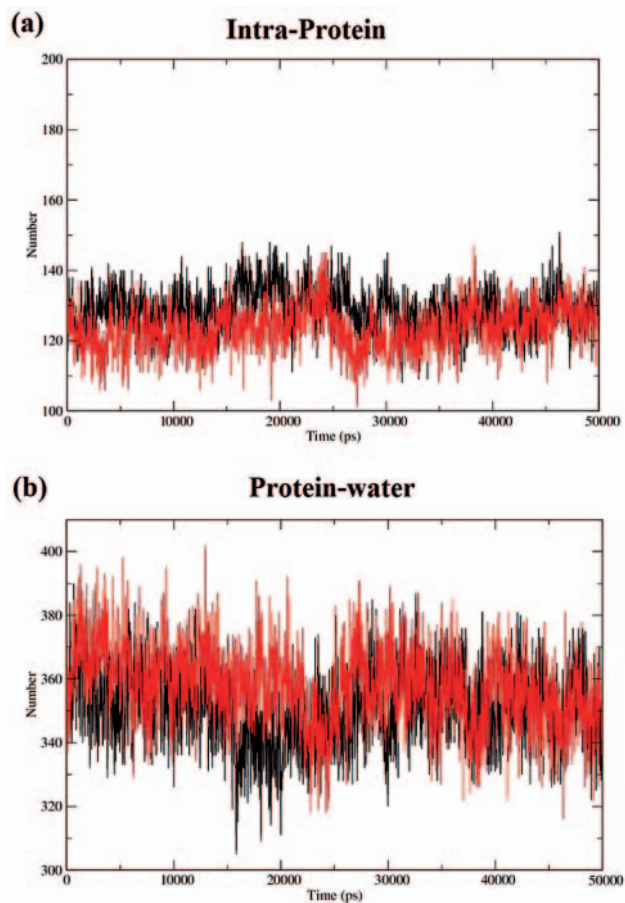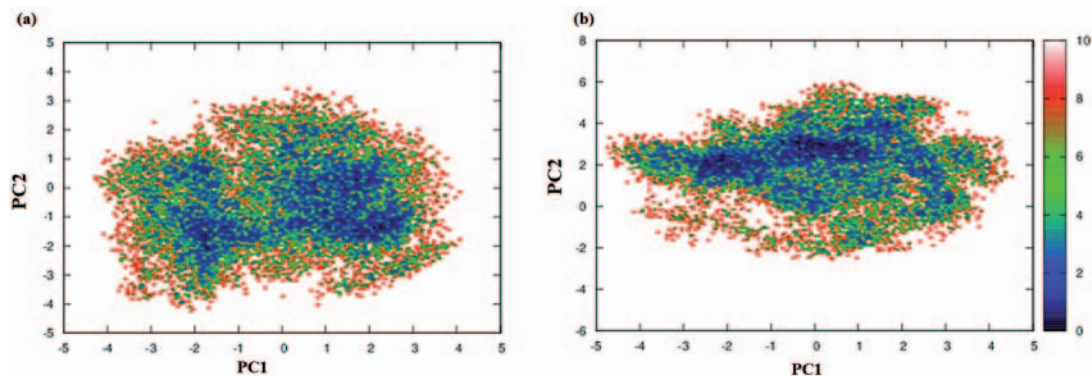
(a)

(b)

Figure 7. — 2D representation of Free Energy landscape of PC1 versus PC2 of (a) native Kras and (b) mutant Kras.

tuating, the mutation other than effecting the region of occurrence is showing its effect overall. The analysis is showing the mutant structure to be more unstable in terms of fluctuations, giving us an insight into the change in the fluctuation pattern between the structures. The significant change in fluctuation can be observed in Mu structure at residue 34, 47, 136, and 157.

After RMSF, change in radius of gyration between the two structures was calculated using g_gyrate tool. The tool analyzes the shape of the protein over time, in Figure 5(a) the black represents the native structure and red the mutant; Figures 5(b) and 5(c) are the representation of Radii of gyration of native and mutant structure over the three axes. The analysis of Rg is showing the mutant structure to be more compact than native Kras.

To further understand the effect of the G12V mutation on Kras, g_hband tool was used. The intra-protein and protein-water hydrogen bond pattern over time was studied. The native protein is forming 128.745 out of 63622.5 possible average number of intra-protein hydrogen bonds per timeframe, while as mutant is forming 123.328 out of 63622.5 possible, showing the decrease as represented in Figure 6(a). The situation is differing when we observe the protein-water hydrogen bond pattern between the two, the native protein 351.249 out of 4.00349e+07 and mutant protein is forming 357.663 out of 3.99991e+07 possible as shown in Figure 6(b).

g-covar and g_anaeig tools were used for understanding the effect of this mutation on global correlated motions in atomic simulations. The Free Energy landscape of the same was calculated using g_sham. The plot shown in Figure7 was plotted using gnuplot. It depicts the projection of principal component 1 versus principle component 2 of both structures. Figure7(a) representing native and Figure7(b) representing mutant structure movement, respectively; the cluster obtained from wt structure is stable, whereas the projection of first two PC of both mutants covers a large area.

Conclusion

The amino acid variation from G to V in Kras is damaging the native conformation. The mutation is the most damaging among the mutations found at codon 12 and 13. The change in RMSD and Rg is conclusively defining the change in conformation of Kras mutant structure. The change in RMSF in mutant structure is also confirming the variation in structural dynamics. These changes can be pivotal in varying the GTPase activity, which has ultimately caused cancer associated phenotypes.

References

[1] International Agency for Research on Cancer: "GLOBOCAN 2012: estimated cancer incidence, mortality and prevalence worldwide in 2012". World Health Organization. Available at: http://globocan.iarc.fr/Pages/fact_sheets_cancer.aspx.

[2] Wright A.A., Howitt B.E., Myers A.P., Dahlberg S.E., Palescandolo E., Van Hummelen P., *et al.*: "Oncogenic mutations in cervical cancer: genomic differences between adenocarcinomas and squamous cell carcinomas of the cervix". *Cancer*, 2013, *119*, 3776.

[3] Cao Z.Y.: "China obstetrics and gynecology". 2nd ed. Beijing: People's Health Press, 2012.

[4] Shi J.F., Qiao Y.L., Smith J.S., Dondog B., Bao Y.P., Dai D., *et al.*: "Epidemiology and Prevention of Human Papillomavirus and Cervical Cancer in China and Mongolia". *Vaccine*, 2008, *26*, M53.

[5] Hakama M., Miller A.B., Day N.E.: "Screening for Cancer of the Uterine Cervix: from the IARC Working Group on Cervical Cancer Screening and the UICC Project Group on the Evaluation of Screening Programmes for Cancer". WHO (Geneva), IARC (Lyon), and UICC (Geneva) 1986, 1–315. IARC Sci. Publ. 76.

[6] Iida K., Nakayama K., Rahman M.T., Rahman M., Ishikawa M., Katagiri A., *et al.*: "EGFR gene amplification is related to adverse clinical outcomes in cervical squamous cell carcinoma, making the EGFR pathway a novel therapeutic target". *Br. J. Cancer*, 2011, *105*, 420.

[7] Janku F., Lee J.J., Tsimberidou A.M., Hong D.S., Naing A., Falchook G.S., *et al.*: "PIK3CA mutations frequently coexist with RAS and BRAF mutations in patients with advanced cancers". *PLoS One*, 2011, *6*, e22769.

[8] Bertelsen B.I., Steine S.J., Sandvei R., Molven A., Laerum O.D.: "Molecular analysis of the PI3K-AKT pathway in uterine cervical neoplasia: frequent PIK3CA amplification and AKT phosphorylation". *Int. J. Cancer*, 2006, *118*, 1877.

[9] McIntyre J.B., Wu J., Craighead P.S., Phan T., Köbel M., Lees-Miller S.P., *et al.*: "PIK3CA mutational status and overall survival in patients with cervical cancer treated with radical chemoradiotherapy". *Gynecol. Oncol.*, 2013, *128*, 409.

[10] Kim T.J., Lee J.W., Song S.Y., Choi J.J., Choi C.H., Kim B.G., *et al.*: "Increased expression of pAKT is associated with radiation resistance in cervical cancer". *Br. J. Cancer*, 2006, *94*, 1678.

[11] Pappa K.I., Choleza M., Markaki S., Giannikaki E., Kyroudi A., Vlachos G., *et al.*: "Consistent absence of BRAF mutations in cervical and endometrial cancer despite KRAS mutation status". *Gynecol. Oncol.*, 2006, *100*, 596.

[12] Kang S., Kim H.S., Seo S.S., Park S.Y., Sidransky D., Dong S.M.: "Inverse correlation between RASSF1A hypermethylation, KRAS and BRAF mutations in cervical adenocarcinoma". *Gynecol. Oncol.*, 2007, *105*, 662.

[13] Jancík S., Drábek J., Radzioch D., Hajdúch M.: "Clinical relevance of KRAS in human cancers." *J. Biomed. Biotechnol.*, 2010, *2010*, 150960. doi: 10.1155/2010/150960. Epub 2010 Jun 7.

[14] Stenzel A., Semczuk A., Rózyńskal K., Jakowicki J., Wojcierowski J.: "Low-risk" and "high-risk" HPV-infection and K-ras gene point mutations in human cervical cancer: a study of 31 cases". *Pathol. Res. Pract.*, 2001, *197*, 597.

[15] García, Dabeiba Adriana, Yazmín Rocío Arias, and Fabio Ancízar Aristizábal. "Detection of genes mutations in the K-ras, H-ras and EGFR in samples of blood plasma and cervical smears for patients with cervical intraepithelial neoplasia III and cervical cancer". *Colombia Médica*, 2009, *40*, 34.

[16] Mammas I.N., Zafiropoulos A., Koumantakis E., Sifakis S., Spandidos D.A.: "Transcriptional activation of H- and N-ras oncogenes in human cervical cancer". *Gynecol. Oncol.*, 2004, *92*, 941.

[17] Pappa K.I., Choleza M., Markaki S., Giannikaki E., Kyroudi A., Vlachos G., *et al.*: "Consistent absence of BRAF mutations in cervical and endometrial cancer despite KRAS mutation status". *Gynecol. Oncol.*, 2006, *100*, 596.

[18] Kang S., Kim H.S., Seo S.S., Park S.Y., Sidransky D., Dong S.M.: "Inverse correlation between RASSF1A hypermethylation, KRAS and BRAF mutations in cervical adenocarcinoma". *Gynecol. Oncol.*, 2007, *105*, 662.

[19] Wegman P., Ahlin C., Sorbe B.: "Genetic alterations in the K-Ras gene influence the prognosis in patients with cervical cancer treated by radiotherapy". *Int. J. Gynecol. Cancer*, 2011, *21*, 86.

[20] MacConaill L.E., Campbell C.D., Kehoe S.M., Bass A.J., Hatton C., Niu L., *et al.*: "Profiling critical cancer gene mutations in clinical tumor samples". PLoS One. 2009; 4(11):e7887.

[21] Cibulskis K., Lawrence M.S., Carter S.L., Sivachenko A., Jaffe D., Sougnez C., *et al.*: "Sensitive detection of somatic point mutations in impure and heterogeneous cancer samples". *Nat. Biotechnol.*, 2013, *31*, 213.

[22] Kumar P., Henikoff S., Ng P.C.: "Predicting the effects of coding non-synonymous variants on protein function using the SIFT algorithm". *Nat. Protoc.*, 2009, *4*, 1073.

[23] Adzhubei I.A., Schmidt S., Peshkin L., Ramensky V.E., Gerasimova A., Bork P., Kondrashov A.S., Sunyaev S.R.: "A method and server for predicting damaging missense mutations". *Nat. Methods*, 2010, *7*, 248.

[24] Capriotti E., Calabrese R., Casadio R.: "Predicting the insurgence of human genetic diseases associated to single point protein mutations with support vector machines and evolutionary information". *Bioinformatics*, 2006, *22*, 2729.

[25] Li B., Krishnan V.G., Mort M.E., Xin F., Kamati K.K., Cooper D.N., *et al.*: "Automated inference of molecular mechanisms of disease from amino acid substitutions" *Bioinformatics*, 2009, *25*, 2744.

[26] Ostrem J.M., Peters U., Sos M.L., Wells J.A., Shokat K.M.: "K-Ras (G12C) inhibitors allosterically control GTP affinity and effector interactions". *Nature*, 2013, *503*, 548.

[27] Hess B., Kutzner C., Van Der Spoel D., Lindahl E.: "GROMACS 4: Algorithms for highly efficient, load-balanced, and scalable molecular simulation". *J. Chem. Theory Comput.*, 2008, *4*, 435.

[28] Accelrys Software Inc.: "Discovery Studio Modeling Environment, Release 3.5". San Diego: Accelrys Software Inc., 2012.

[29] Berendsen H.J.C., Postma J.P.M., van Gunsteren W.F., Dinola A., Haak J.R.: "Molecular dynamics with coupling to an external bath". *J. Chem. Phys.*, 1984, *81*, 3684.

[30] Cheatham T.E., Miller J.L., Fox T., Darden T.A., Kollman P.A.: "Molecular dynamics simulations on solvated biomolecular systems: the particle mesh ewald method leads to stable trajectories of DNA, RNA, and proteins". J. Am. Chem. Soc. 1995, *14*, 4193.

[31] Humphrey W., Dalke A., Schulten K.: "VMD: visual molecular dynamics". *J. Mol. Graph.*, 1996, *14*, 33.

[32] Turner P. J.: "XMGRACE, Version 5.1.19". Center for Coastal and Land-Margin Research, Oregon Graduate Institute of Science and Technology, Beaverton, OR, 2005.

Address reprint requests to:
S.M. FU, M.D.
Central Laboratory
The People's Hospital of Hainan Province
No.19, Xiuhua Road, Xiuying District
Haikou, Hainan 570311 (China)
e-mail: fushengmiao@gmail.com